GLOMERULAR SIGNALS UNDERLYING OLFACTORY NAVIGATION

By

Nelly Merveille Nouboussi Nkenfack

A THESIS

Presented to the Department of Biology
and the Robert D. Clark Honors College
in partial fulfillment of the requirements for the degree of
Bachelor of Science

May 2020

An Abstract of the Thesis of

Nelly M. Nouboussi Nkenfack for the degree of Bachelor of Science
in the Department of Biology to be taken in June 2020

Title: GLOMERULAR SIGNALS UNDERLYING OLFACTORY NAVIGATION

Approved: _____*Dr. Matt Smear*_____
Primary Thesis Advisor

The olfactory system is the least-studied sense, although it plays key roles in different aspects of our existence. Our lab and others have examined the behavioral structure of olfactory navigation and have found that mice use a combination of serial and stereo cues to locate the source of an odor. Our next goal is to compare sampling movements directly against sensory input in freely moving mice in order to establish a correlation between sensory input and mouse behavior. Most imaging studies have been conducted on restrained mice, which allows for better control. However, animals behave differently when restrained, and specific behavioral dynamics can only be studied when the animal can move naturally in the environment. The first step in this goal, which is the topic of this project, is to successfully express fluorescence indicators in the olfactory bulb and to detect this expression using our imaging apparatus. For this purpose, we have been troubleshooting the surgical and imaging techniques necessary to begin our experiments. To achieve the expression of our fluorescence sensor GCaMP, we either injected a virus encoding the fluorescence protein into mice brains or engineered mice to encode the sensor gene in their genome. Histology revealed that we successfully expressed GCaMP in some mice, while we could only observe background fluorescence in others. This could result from the frying of the bulb due to continuous expression of the protein or degradation of the virus. Despite the difficulty of the surgeries, we could visualize activity in the glomeruli of live mice with the two-photon microscope, although our success rate remains low. We are continuously adjusting our protocol to improve our techniques, so we can move on to the next stage of our project.

Acknowledgements

I would like to thank Dr. Matt Smear for giving me the opportunity to work in his lab at the end of freshman year and for always taking the time to answers all my questions and to guide me through this project. Throughout my time as research assistant in the Smear lab I've learned so much about how research is conducted, including some of the challenges researchers face. I also want to thank my mentor Amanda Welch for walking me through individual techniques and guiding me through the different steps of this project. I would also like to thank Dr. Morgan Brown and Teresa Findley for allowing me to work under their supervision during my time in the lab. I would also like to thank Blake Holcomb for helping me when I sent him multiple text messages and emails with various questions about my project, and for being a mentor and friend in the lab. I would also like to thank Dr. Elizabeth Raisanen for serving on my committee and for her advice and support when I complained about the challenges. I am grateful for the Clark Honors College for giving me the opportunity to explore my research interest and for the numerous support it provided through its faculty members. Finally, I must express my gratitude to the almighty God for giving me the strength to pursue this project and to my family and friends who have never stopped encouraging me during my college career.

Table of Contents

List of Tables and Figures

Introduction:

The ability of an animal to detect and respond to changes in the environment is critical for its survival. Such an ability is especially important for the animal to maintain homeostasis, to escape dangerous situations, and to adapt to new environments. However, animals differ in the sensory system most used in their day-to-day experiences. For example, humans and other animals greatly rely on their visual system and to a lesser extent on their auditory system. Mice on the other hand, have a developed olfactory system and rely less on their visual system.

The olfactory system is the least-covered sensory system in neuroscience classes. However, it plays an important role in many aspects of our existence, and thus should be studied extensively. Attraction to other humans is especially reliant on olfaction as we are more likely to form close bonds to people whom we perceive as smelling good. Food intake is also reliant on the olfactory system because flavor is non-existent without olfaction. This is why food is not as delicious when we have a cold, as it interferes with our ability to detect chemicals released by the food. The ability to smell is also important for our survival because a food's smell can be an indication of how healthy it is. Unpleasant smells prevent us from ingesting spoiled and thus harmful food products. Additionally, impaired olfactory function has been a marker for depression (Negoias et al., 2010; Croy et al., 2013). Beyond its importance to humans, the olfactory system is the most prominent sense in many animal species. Dogs, for example, have been shown to rely more on their olfactory system than the visual system even in conditions of high light intensity (Gazit and Terkel, 2003). Other animals that rely on olfaction include mice and Eastern American Moles. Finally, studying the olfactory system is important because it gives insight into general brain function. Connections can be made between how the olfactory system works and other sensory systems such as the vision and auditory systems.

Anatomy of the Olfactory System

Much is known about the general anatomy of the olfactory system in mammals. Odor molecules bind to receptors located on the surface of olfactory receptor neurons (ORN) located in the olfactory epithelium, within the nasal cavity (figure 1). ORN act as the sensory transducers, because they convert the chemical information in the odor molecules into electrical impulses in the form of action potentials. Each ORN can only express one type of receptor. There are approximately 1000 receptor genes in the mouse genome (Wilson and Mainen, 2006). ORN project into structures called glomeruli (GL), which are located in the olfactory bulb. Each glomerulus is specific to one type of ORN (Mori et al, 1999). Within the glomeruli, ORN make excitatory synapses with the mitral and tufted cells (M and T), which are the output neurons of the olfactory bulb. They send the information to the olfactory cortex, where it is processed in order for us to respond appropriately.

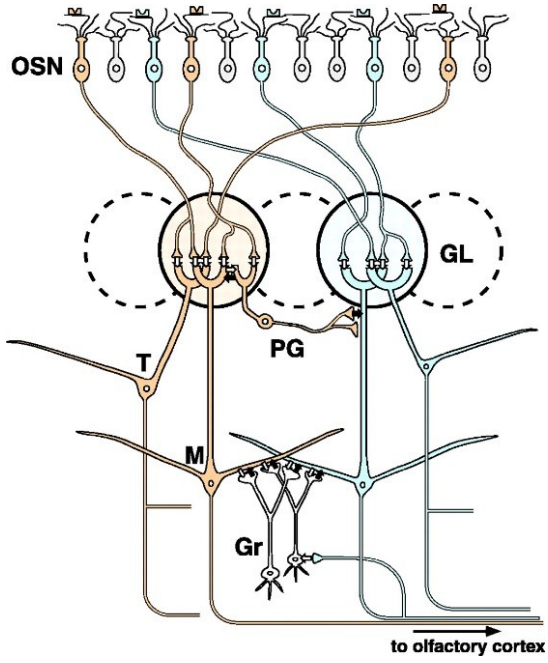

Figure 1. Olfactory bulb circuitry. The mammalian olfactory bulb is composed of multiple types of neurons including the olfactory sensory neurons (OSN), the mitral and tufted cells (M and T). Periglomerular cells (PG) and granule (Gr) cells are interneurons that modify signal transmission through the olfactory bulb. (Mori et al., 1999)

Mice are an important model organism for the study of the olfactory system because they have one of the most developed olfactory systems, containing more receptor genes than humans (~1000 for mice and ~350 for humans) (Wilson and Mainen, 2006). Additionally, the olfactory bulb in rodents like mice is easily accessible for studies. However, the most significant motivation for working with mice is the availability of genetic tools. For a long time mice were the only mammals in which genetic engineering was feasible. Thus, scientists were able to genetically engineer mice to express different indicators in very specific regions to study specific processes. Since then, mice have been the dominant model organism for systems neuroscience.

While the general anatomy of the olfactory system has been elucidated, very little is known about how the olfactory system provides the navigational cues necessary for localizing odors. The mechanism underlying olfactory processing remains unclear: what is the pattern of activity of neurons within the glomeruli when the mouse is exposed to an odor source? How does this pattern of brain activity affect subsequent odor sampling?

Literature review**:**

Behavioral Structure of Olfactory Search

Understanding the behavioral structure of olfactory search is very important because it lays the groundwork for determining brain circuits underlying olfactory navigation. This has been examined using different animal models such as moles and mice. Kenneth Catania studied blind Eastern American moles (*Scalopus aquaticus*), which have degenerated mechanoreceptive organs compared to other moles, and small ears that detect lower frequencies. Thus, they were expected to not be able to localize prey efficiently. However, it was discovered that they are very efficient at detecting food and rely extensively on their olfactory system. Catania thus used them as an animal model in different search paradigms. He found that they were able to localize the prey within 5 seconds of the trial initiation. He reasoned that the accuracy of the animals and the direct path taken toward the food suggest that they are using bilateral cues (Catania, 2013). Bilateral cues refer to the information that animals gain from the difference in odor concentration entering each nostril.

In order to determine the contribution of bilateral cues, he performed nostril occlusions in which airflow was blocked through one nostril at once. He found that while they were still able to locate the food, they spent more time searching and their path was not as direct. To further test the importance of bilateral cues, he inserted tubes inside their nose and crossed the airflow. Thus, the right nostril sampled the left side and vice versa. This completely disoriented the moles and they were never able to find the food. From his experiments, Catania proposed a model to explain the contribution of different cues to olfactory search. He hypothesized that serial spatial cues are used at distant locations from the source where the gradient is shallow. The animal can make large movements to sample large areas to get directional information. However, at closer

distances where the gradient is steep, shorter movements and bilateral comparisons provide additional cues (Catania, 2013). Thus, the animal compares the concentration of odor at different locations when farther from the odor source but compares the concentration of odors in each nostril when closer to the odor source.

Peter Jones and Nathan Urban performed similar experiments in mice but also examined the turns mice make as they move along a trail. They found that mice make turns at oblique angles which take them back and forth along the trail length, and use information about the most recent sniffs to determine the magnitude of the next turn (Jones and Urban, 2018). From the nostril occlusion experiments, they found that mice shift the position at which they turn back toward the trail, and typically shift toward the open nostril. This led them to conclude that mice use stereo cues (bilateral cues) for precise, millimeter-scale localization of odor source (Jones and Urban, 2018). Thus, both studies discussed above determined that bilateral cues are very important for localization of odor in small scales, and especially when the animal is very close to the odor source.

Neural Coding

The nature of neural coding of olfactory information has also received some attention. In their review article, Brett Johnson and Michael Leon (2007) specifically examined how odor molecules with various chemical structures are coded in the olfactory bulb of rats. They characterized different odor molecules based on the number of carbons in the chain, the bond saturation, and aromaticity. They found that nearby glomeruli within the olfactory bulb react to odorants of similar chemical characteristics (Johnson & Leon, 2007). Thus, similar molecules are encoded in similar locations.

Wesson et al. (2009) studied the relationship between the sniff frequency, odorant discrimination, and receptor sensory neuron activity in rats. The objective of this study was to determine if an increase in sniff frequency during sampling behavior has an influence on the neural coding of olfactory information. They observed an increase in sniff frequency before and after the activation of olfactory sensory neurons. The conclusion drawn from this research shows that an increase in sniff frequency is not directly involved in the processing of information but merely allows the animal to acquire the stimulus more quickly (Wesson et al., 2009). In other words, the increase in sniffing simply acts to increase the rate at which the mice sample odorant molecules. Urvashi Battacharyya and Upinder Singh Bhalla (2015) also detected an increase in sniff frequency but a decrease in the moving pace of mice during the sampling of odor molecules. These two studies show that rodents alter their behavior during the sampling of odorants in order to maximize the efficiency of detection of the odor molecules and thus the accuracy of discrimination.

Limitations of Restraining Mice

The research conducted by Wesson et al., as well as Bhattacharyya and Bhalla, studies one of two things at a time: 1) the relationship between neural activity and behavioral patterns in restrained mice, or 2) a behavior alone of freely-moving mice. Wesson et al. (2009), for example, measured the sniffing rate and imaged the olfactory bulb of mice that are head-fixed in order "to eliminate confounds of locomotion." While restraining enables better stimulus control and recording clarity, it induces unnatural behavior. Wallace et. al (2013) found that rats move their nose differently when head-fixed than when freely-moving. O'Connor et al. (2010) found that head-fixed mice position their whiskers in a manner that has been associated with rewards,

which has not been observed in unrestrained mice. Furthermore, rodents breathe differently when freely moving than when restrained (Wesson, Verhagen & Wachowiack, 2009). Finally, restraining mice eliminates head-movement, which is an important feature of multiple odor-guided behaviors including trail following (Khan et al., 2012; Jones and Urban 2018), plume tracking (Bhattacharyya & Bhalla, 2015; Catania, 2013), courtship (Neunuebel et al., 2015), and competitive scent marking (Hurst and Beynon, 2004). Since imaging studies have focused on restrained mice, it is not likely that the findings will generalize to freely-moving mice.

Genetically Encoded Neural Activity Indicators

Some of the studies mentioned above have employed imaging techniques to study how olfactory information is coded in the brain. Various techniques were used such as 2-deoxyglucose staining (Johnson and Leon, 2007; Stewart et al., 1979), intrinsic signal imaging (Meister & Bonhoeffer, 2001; Soucy et al., 2009;), dye imaging (Spors & Grinvald, 2002;), and imaging of genetically encoded indicators (Kass et al., 2013; Kato et al., 2012). While these techniques can reveal spatial patterns of activity, they cannot capture glomerular activity in freely-moving mice, which requires higher temporal resolution.

Multiple genetically encoded neural activity indicators (GENAI) have been developed over the years for brain imaging studies. They use various mechanisms of action. Some report the concentration of calcium, while others respond to changes in voltage or report the concentration of neurotransmitters at synapses (Luo et al., 2018). During an action potential, the voltage of a neuron decreases, calcium enters the cell and causes vesicles containing neurotransmitters to release them into the synapse. Thus, all three mechanisms of action of these GENAI can indicate neural activity. GENAI measure a property called the contrast (*C*), which is

the change in intensity between two locations on the image divided by the average image brightness, as shown in the following equation (Luo et al., 2018):

$$C = \frac{I^1 - I^0}{I} = \frac{\Delta I}{I}$$

It is important to have an indicator that has a high signal-to-noise ratio because it will detect minor changes in intensity despite a high background firing. GENAI also have high temporal resolution, which means they have high precision with respect to time (Luo et al., 2018). In other words, they have a high frequency of sampling and are thus able to detect rapid changes in firing intensity. GCaMP6f, which was used in the Lerman et al. study (2016), is a type of calcium indicator that is composed of GFP (Green-fluorescent protein) and the calmodulin (CaM) and M13 domains (Luo et al., 2018). When these domains bind calcium, the whole protein changes conformation, which triggers fluorescence emission by GFP (Luo et al., 2018). While both GCaMP6f and GCaMP7f sensors both have fast kinetics, GCaMP7f has been found to show substantially better performance in vivo and in vitro (Dana et al., 2019). In this project, we will be using both GCaMP6f and GCaMP7f sensors.

Research Aims**:**

Our lab and others have examined the behavioral structure of olfactory navigation. Our next goal is to compare sampling movements directly against sensory input in freely moving mice. In most sensory neuroscience paradigms, mice are restrained, which allows for more controlled conditions, but this approach is limiting because it cannot reveal how sensory systems operate when the mouse is unrestrained. Our lab has found through our behavioral assay that mice develop a consistent repertoire of sniff-synchronized movements, and these behavioral dynamics can only be studied when the animal can move naturally in the environment. We aim to examine how incoming olfactory signals shape the structure of navigational behavior.

For this purpose, we will develop methods to monitor and mimic olfactory bulb input during free movement through noisy odor gradients. In order to monitor olfactory input to the brain, we will combine our behavioral assay with imaging. We will express genetically encoded fluorescence indicators to visualize glomerular input during sampling movements. This will allow us to determine how navigating an odor gradient drives glomerular activity. Our technique will enable us to establish a relationship between sensory input and mouse behavior. We hypothesize that the structure of navigation behavior depends on sniff-to-sniff comparison of sensory input. Movement structure will depend not only on the most recent sniff, but on changes between successive sniffs.

Specific Thesis Aim:

Our research aim involves combining our behavioral assay with imaging, which requires us to express genetically encoded fluorescence indicators in the brain. The first step in this goal is to successfully express the fluorescence indicators in the olfactory bulb and to detect this expression using our imaging apparatus. The goal of this project is to troubleshoot the surgical

and imaging techniques necessary to begin our experiments. During the troubleshooting period, experiments are done on restrained mice, although the ultimate goal is to image freely-moving mice. If experiments were run in freely-moving mice initially and did not work, we would not know if the problem results from fluorescent indicator not being sensitive enough or if there is an issue with the imaging technology. From there we will image freely moving mice performing olfactory search in a new behavioral assay (Figure 2). In this set-up, mice will be imaged from the bottom to prevent obstruction of tracking via the cable used to monitor sniffing (Smear Lab unpublished). The floor is reflective for the mice to prevent fearful responses. This project is important and novel because it is the first step in developing a method that will allow the lab to capture glomerular signals in unrestrained mice. As mentioned above, most imaging studies have been done on restrained mice, which significantly limits the extent to which olfactory processing can be studied. Future studies can use this technique to determine the mechanisms behind olfactory processing.

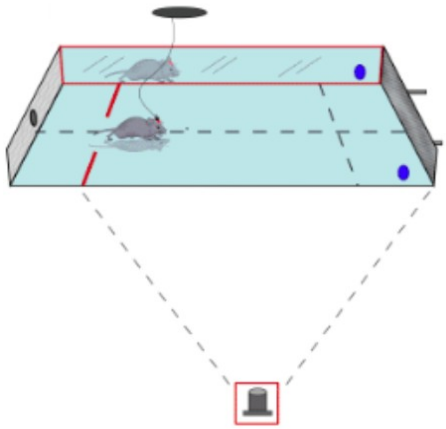

Figure 2: New Behavioral Assay. Mice are presented with a two-choice search task where they have to search up a concentration gradient. Trials begin when mice cross the red line after the initiation poke. They will be imaged from the bottom, using fiber photometry. *Figure from Smear Lab unpublished.*

Materials and Methods

The viruses:

To visualize the activity of neurons within the olfactory bulb, we injected viral vectors encoding fluorescent calcium sensors into the olfactory bulb of different mice strains. Two different viruses are used in the experiments. The first virus is called AAV jGCaMP7f (or GCaMP7f) which is non-specific and non-Cre dependent, meaning it can be expressed in any cell. The second virus is called AAV jGCaMP7f-FLUX (or GCaMP7f-FLUX) and is Cre-dependent. The GCaMP7f-FLUX virus contains a plasmid in which the promoter is inverted (Figure 3). The enzyme Cre recombinase acts to reverse the gene so that it can be expressed (Figure 3). Thus, only cells containing the Cre recombinase enzyme will be able to express this gene. The GCaMP protein encoded by both viral vectors consists of the Green fluorescent protein (GFP), the calcium-binding protein calmodulin (CaM), and the CaM interacting M13 peptide. Upon calcium (Ca^{2+}) binding, conformational changes in CaM and M13 cause GFP to fluoresce significantly more than basal level. Because calcium enters the cell during an action potential, levels of fluorescence correlate with activity within the olfactory bulb.

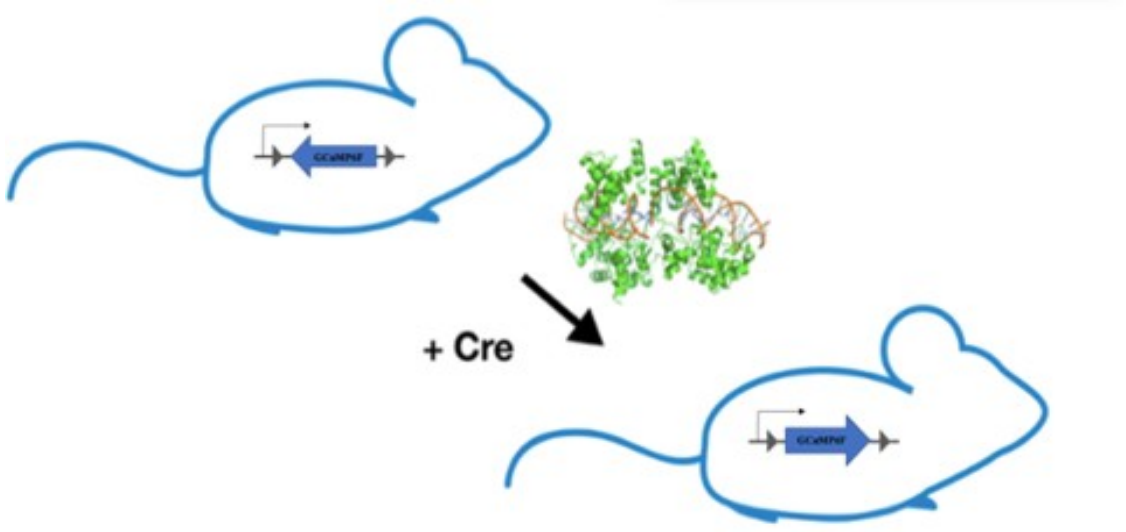

Figure 3. The effect of the Cre recombinase protein on the expression of GCaMP7F

Mouse Strains:

Three mouse strains were used in these experiments. B6 mice are wild type and were injected with the non-specific virus which should result in widespread expression throughout the olfactory bulb. Tbet-cre mice express the Cre recombinase protein specifically in the mitral and tufted cells. They were injected with the Cre-dependent virus, which should restrict expression of GCaMP to the mitral and tufted cells. The third line of mice results from crossing Tbet-cre mice with Ai148(TIT2L-GC6f-ICL-tTA2)-D or Ai148D mice. Ai148D mice harbor a TIGRE-Ins-TRE2-LSL-GCaMP6f-Ins-CAG-LSL-tTA2 conditional allele, which contains a TRE promoter, a STOP cassette flanked by loxP sites and GCaMP6f sequence, followed by a CAG promoter, a STOP cassette flanked by lox2272 sites and a tTA2 sequence (Figure 4A). TIGRE is an intergenic region on mouse chromosome 6 that allows expression to be tightly regulated (The Jackson Laboratory). In Ai148D mice, the STOP cassettes prevent the transcription of the GCaMP6f and tTA2 genes. The Cre recombinase protein is necessary to delete the STOP cassettes, allowing expression of these genes (Figure 4B). In our experiment, Ai148D mice were bred with Tbet-cre mice that express the Cre recombinase protein in the mitral and tufted cells.

The resulting mouse line is Tbet-cre - Ai148D, which can express GFP in mitral and tufted cells (Figure 4B). We did not perform virus injections on these mice because they already contain the GCaMP gene in their genome. Expression of Cre recombinase in these mice can be regulated through their diet. Doxycycline, an analog of tetracycline, prevents Cre recombinase from excising the LoxP sites, thus preventing the expression of our gene of interest. Because we did not feed Doxycycline to the mice, they should be able to express GCaMP throughout their lives.

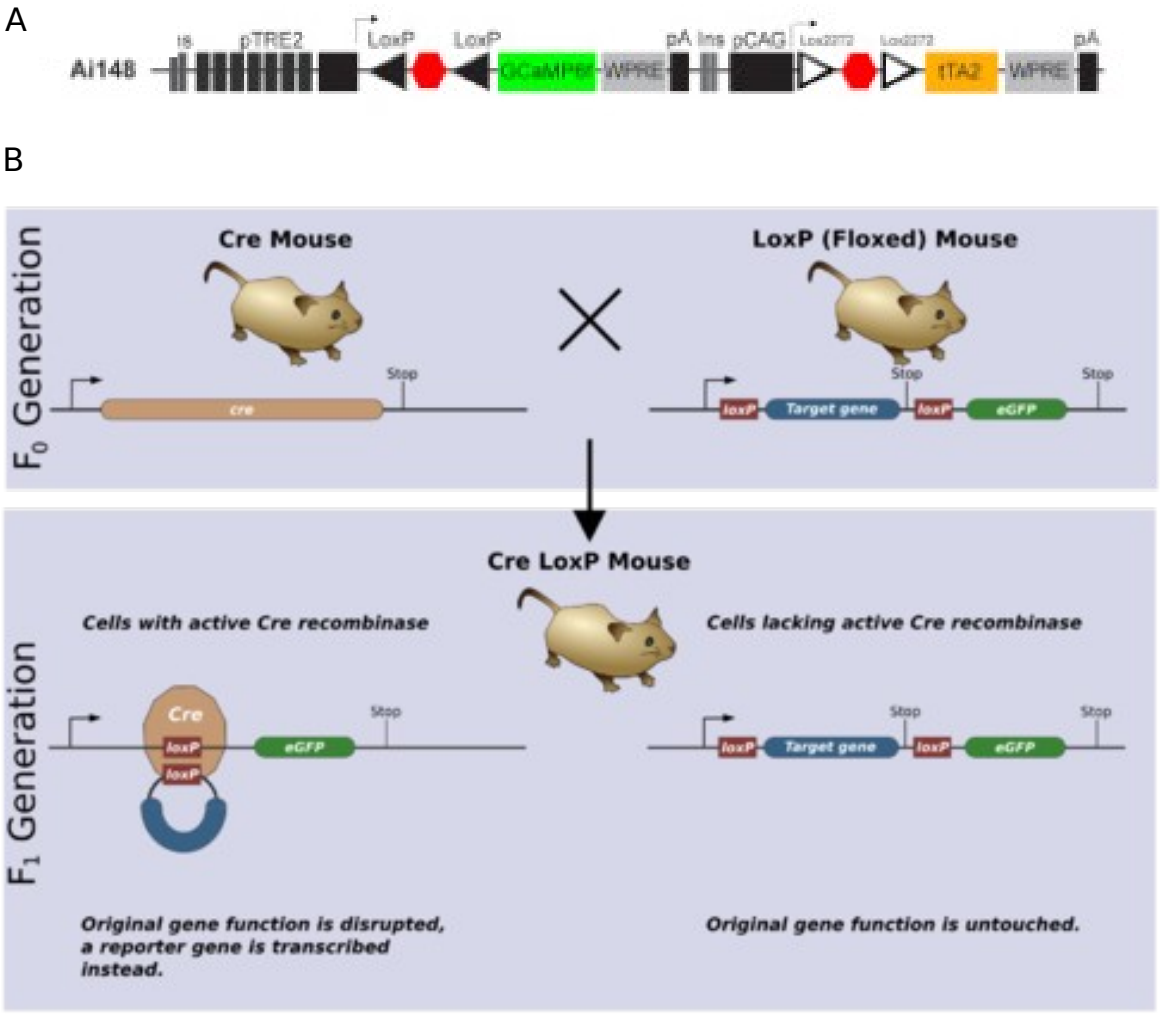

Figure 4. Cre-dependent expression of GCamp in Tbet-cre – Ai148D mice. **A.** Schematic diagram of the conditional allele in the Tbet-Cce – Ai148D mice genome (Daigle et. al, 2017). **B.** Representative diagram of crossing Tbet-cre (Cre Mouse) with Ai148D mice (LoxP floxed) mouse (Zepper, 2008). In this diagram the target gene is the equivalent to the STOP cassette in part A and the eGFP gene is equivalent to the GCaMP6F. When these mice are crossed, cells expressing the Cre recombinase enzyme will express GCaMP6F.

Animal Care and Housing:

All experimental procedures are part of the Smear lab's protocol, which has been approved by the University of Oregon's Institutional Animal Care and Use Committee (IACUC) and is in compliance with the National Institute of Health Guide to the Care and Use of Laboratory Animals. B6 (n = 18) Tbet-cre (n = 5) and Tbet-cre - Ai148D (n = 4) mice from the Terrestrial Animal Care Services (TeACS) used in these experiments were 8 weeks or older. They were group-housed (up to 4 mice per cage) in plastic cages to ameliorate surgery recovery outcomes. Plastic cages contained bedding and running wheels provided by the TeACS. Mice were fed standard rodent chow *ad libitum* and received unlimited chlorinated water. Tbet-Cre - Ai148D mice were never fed doxycycline or tetracycline. After surgery, mice were put in a new cage and were group-housed based on their surgery date. Their health was monitored daily and more extensively during the three days post-surgery.

Surgical Procedures:

During all procedures, animals were anesthetized using 1.5-3% isoflurane. The concentration was adjusted throughout the surgery depending on the state of the animal. Before starting the surgeries, all tools were sterilized using the autoclave machine in the mouse facility. Between surgeries, tools were sterilized with a hot bead sterilizer. After all surgeries, all animals were administered post-op drugs and were allowed to recover in an incubator in the recovery room for 3 days.

Virus injections:

Injections were performed using either the Nanoject or a World Precision Instruments (WPI) 10 μl nanofil syringe. Before starting the surgeries, animals received intravenous injections of the

surgery analgesics buprenorphine (0.1 mg/kg) and subcutaneous injections of meloxicam SR (4mg/kg). We also gave them lactated ringer subcutaneously to keep them hydrated. We shaved and cleaned the incision site and injected Lidocaine subcutaneously above the skull before doing the incision. After the incision, we drilled one or two holes through the skull above the left medial side of the olfactory bulb, anterior to bregma. Drill holes were 120 +/- 3 μm deep from the surface of the skull. We inserted the Nanoject or Hamilton syringe at 0.800 mm from the surface of the brain and injected the virus. Different volumes of virus were injected in different animals, ranging from 400 nL to 800 nL per injection site. The virus was always injected at a rate of 100 nL per minute. We waited for 4 to 8 min to allow the virus to be absorbed before pulling out the syringe. We removed the syringe gradually to avoid damage to the skull and to prevent the virus from being sucked out due to change in pressure. We then sutured the skin on the skull and allowed the animal to recover.

Cranial Window:

Two days before the surgery, we gave the animals intraperitoneal injections of Baytril (10 mg/kg). Additionally, the day before the surgery and 2 hours before on the day of the surgery, we gave them intraperitoneal injections of Baytril and dexomethasone (10 mg/kg), to prevent infection. Before starting the surgeries, we gave them intraperitoneal injections of the surgery analgesics buprenorphine and the anti-inflammatory Mannitol (200 mg/mL). We also gave them lactated ringer subcutaneously to keep them hydrated. We shaved and cleaned the incision site and injected Lidocaine subcutaneously above the skull. After injecting the incision site with lidocaine, we removed the skin to expose the skull. For Tbet-cre mice, we identified the drill holes before outlining the section of the skull to remove. For Tbet-cre - Ai148D mice, we outlined a section of the skull the above the left and right olfactory bulb. The size of the section

of skull varied from approximately $1mm^2$ to $3mm^2$. We applied a layer of synthetic dura over the brain before placing the window. The glass window was secured to the brain with cyanoacrylate. We then placed a 3 cm head bar on the skull behind the animal's ears in order to head-fix the mice during imaging sessions. The head bar was secured with cyanoacrylate. The day after surgery, we gave the mice the analgesic meloxicam-SR. We maintained the health of the skin by debriding and cleaning as necessary. Also, we checked the cranial windows periodically to determine if imaging was possible, as bone regrowth and inflammation often impeded our ability to image certain mice.

Olfactory Assay:

Software: All experiments were run using a combination of custom MATLAB and Bpod scripts. Bpod is an open source software and codes are available upon request.

Sniff recordings: We measured inhalation and exhalation using an external flow sensor located several millimeters from the nostril not receiving odor presentation. We placed the Flo sensor as close to the nostril as possible but avoided direct contact with the nostril to avoid irritating the animal. The signal generated by the flow sensor is equivalent to the more invasive intranasal cannula used by Parabucki et al. (Smear Lab, unpublished).

Image capture: We used widefield and two-photon microscopy to image the olfactory bulb. Two-photon microscopy is a powerful tool to monitor expression of distinct neurons within the brain. It allows for precise spatial and temporal resolution of individual cells at depths located 300 to 600 μm below the surface of the olfactory bulb. During two-photon imaging, high energy light passes through the window of head-fixed mice. Neural activity results in fluorescence emission from the GCaMP expressed in these cells. This fluorescence is filtered and captured using a photomultiplier tube. Widefield microscopy was also used to verify GCaMP7 expression

and kinetics. It has less temporal and spatial resolution than two-photon imaging and thus allows for visualization of the integrated fluorescence emitted from the bulb. It only allows for the identification of neurons roughly 200 μm from the surface.

Histology:
In order to confirm expression of GCaMP in mice, we performed a necropsy to remove the right and left olfactory bulb in the brain of 6 mice. The bulbs were fixed in paraformaldehyde for at least 16 hours. The bulb was cryo-sectioned into 50 μm coronal sections. The sections were DAPI-stained and imaged using a fluorescence microscope.

DIO Assay:
We injected two B6 mice with the lipophilic fluorescent tracer 3,3'-Dioctadecyloxacarbocyanine Perchlorate (figure 5). It belongs to family fluorescent stains used for labeling membranes and other hydrophobic structures. These dyes are weakly fluorescent in water, but their fluorescence is enhanced when incorporated into plasma membranes. Once injected into cells, they diffuse laterally within the plasma membrane, resulting in staining of the entire cell. We injected DIO into the left and right olfactory bulbs of the mice. A day later, we performed a necropsy on the mice and extracted their olfactory bulb. The bulbs were cryo-sectioned and imaged with a fluorescence microscope.

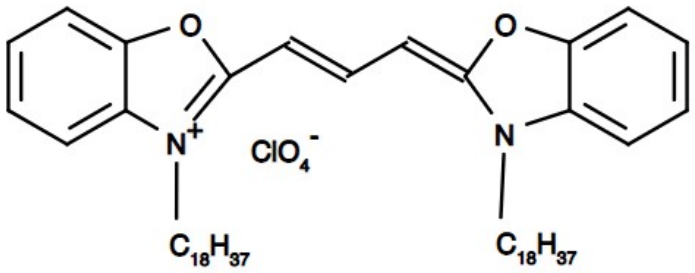

Figure 5. Chemical structure of DiO 3,3'-Dioctadecyloxacarbocyanine Perchlorate (AAT Bioquest).

Table 1 summarizes the experimental details for each mouse strain.

Mouse strain	Description	Virus injected	Surgeries performed	Histology
B6	Wildtype	Non-specific, Cre-independent	Virus Injections, Cranial window	Yes
Tbet-Cre	Expresses the Cre Recombinase protein in the mitral layer	Cre-dependent	Virus Injections, Cranial window	Yes
Tbet-Cre-Ai148D	Contains the GCaMP6f gene in its genome	None	Cranial window	Yes

Results:

Verification of injection location using DIO

To examine the injection destination within the olfactory bulb and the efficiency of our injection apparatus, we injected the fluorescent dye DIO in 2 mice (Figure 6). The sections from our DIO mice confirmed that we injected the substance into the targeted area, but they gave us insightful information about some technical issues with our injection set-up. The second panel shows that fluorescence is localized to two areas in the bulb, even though we only injected one site. The most lateral site is located about halfway between the surface of the bulb and the more medial site. This indicated that some DIO was released from the needle at the halfway mark while we waited for the virus to be absorbed, which is not expected. Additionally, panel 3 shows a strip of DIO along the length of bulb, which is not expected because the needle was only inserted at 800 μm below the surface of the brain. Finally, as shown in panel 4, some DIO was released at the surface of the bulb, which was also not expected. These results showed that our

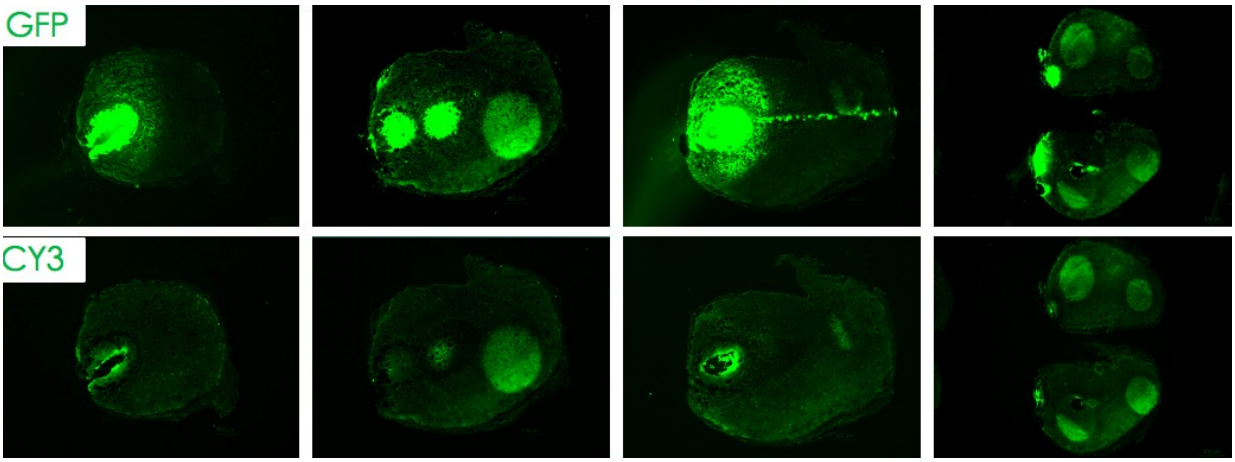

Figure 6: Representative histology sections from DIO mice. Images were obtained with a fluorescence microscope. The top images were obtained using the GFP channel and the bottom images using the Cy3 channel. The Cy3 channel serves as a control because DIO does not absorb light at the frequency emitted in the Cy3 channel. Therefore, fluorescence should not be observed with the Cy3 channel which, for the most part, is the case.

We were not injecting the right amount of solution at the targeted locations, which would be problematic for subsequent experiments. We hoped to restrict expression to the mitral layer and thus needed a specific, controlled, and efficient set-up. As a result, we decided to switch from using the Nanoject set-up to the WPI Syringe, which was also used by another lab at the University of Oregon. Since then, we have been doing injections with the WPI Syringe.

Verification of GCaMP7f expression in B6 Mice and Tbet-cre Mice

We injected the non-specific, non-Cre dependent GCaMP7f virus in B6 mice and the Cre-dependent virus in Tbet-cre mice. To confirm that the virus wa

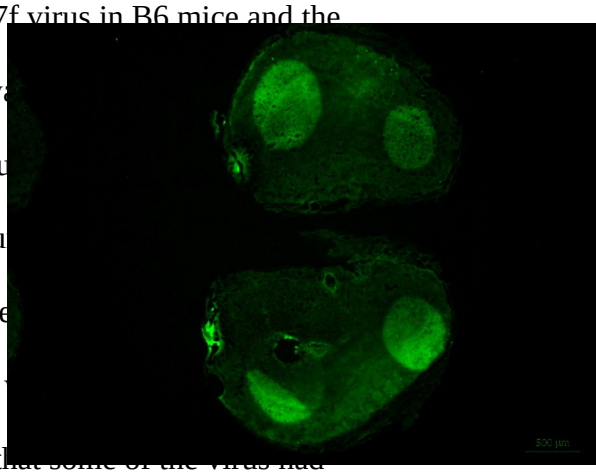

expressed in the olfactory bulb, we looked at sections of the bulb u microscope. GCaMP was successfully expressed in B6 mice (Figu fluorescence is the one present in the GFP images but absent in the mice were injected with the non-specific virus, we expected more GCaMP, but it seems localized to one area. We do see, however, t

begun spreading from the injection site toward the bottom of the bulb (Figure 7, top left panel). The absence of more widespread expression could be an indication that the volume or concentration of virus was too small. We could at least confirm that the virus was expressed in our B6 mice, which was not the case in our Tbet-cre mice (Figure 8). The histological sections from these mice only showed basal fluorescence, which means our virus was not expressed. We expected to see fluorescence along the mitral cell layer, which is highlighted in figure 8B.

Instead, as shown in the top left panel, the image is brightest near the edges. Figure 8B further confirms our assertion that we are seeing basal fluorescence, because while we injected

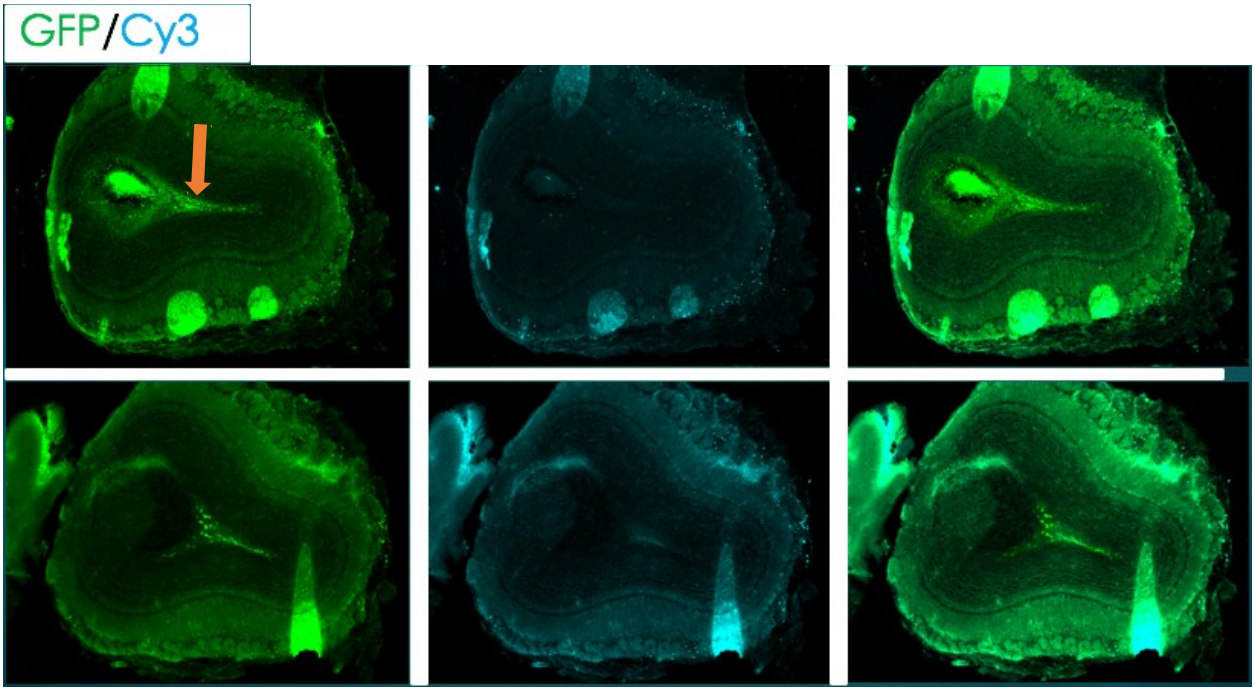

Figure 7: Representative histology sections from B6 mice injected with the GCaMP7F non-specific and non-Cre dependent virus. Images were obtained with a fluorescence microscope using both the GFP channel and the Cy3 channel as a control. Some fluorescence is observed in the GFP channel but none in the Cy3 channel. Arrow points to spread of virus away from the injection location. The lack of widespread GCaMP expression may be due to the small volume of virus injected.

the virus in the left olfactory bulb, both sides of the bulb are equally bright. We expected to see fluorescence in the mitral layer of the left olfactory bulb. There is a distinctly bright spot in the top left olfactory bulb which could be the injection site (Figure 8B). However, it is uncertain

whether that is real fluorescence, because the cells at that spot seem dead (Figure 8B, middle panel). This may be an indication that this region of the bulb was fried over time as a result of the continuous expression of the fluorescence protein. Overall, the results of our virus injections in Tbet-cre mice are definitely not what we expected. This could have resulted from the degradation of the virus over time or the frying of the bulb. These images were obtained almost four months after injection. Thus, the virus might have been degraded by then, or as shown in figure 9B, the bulb might have been fried. Finally, it's also possible that the virus was not successfully injected in the mitral cell layer, explaining why no fluorescence is observed.

A

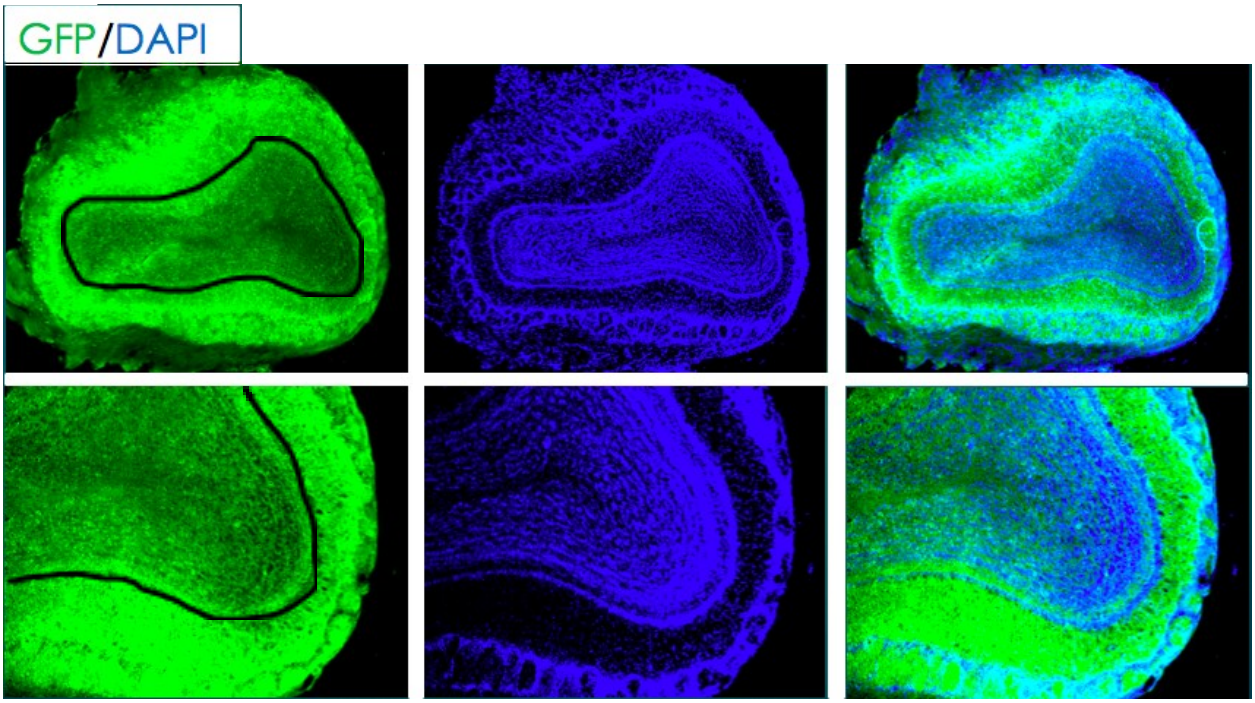

B

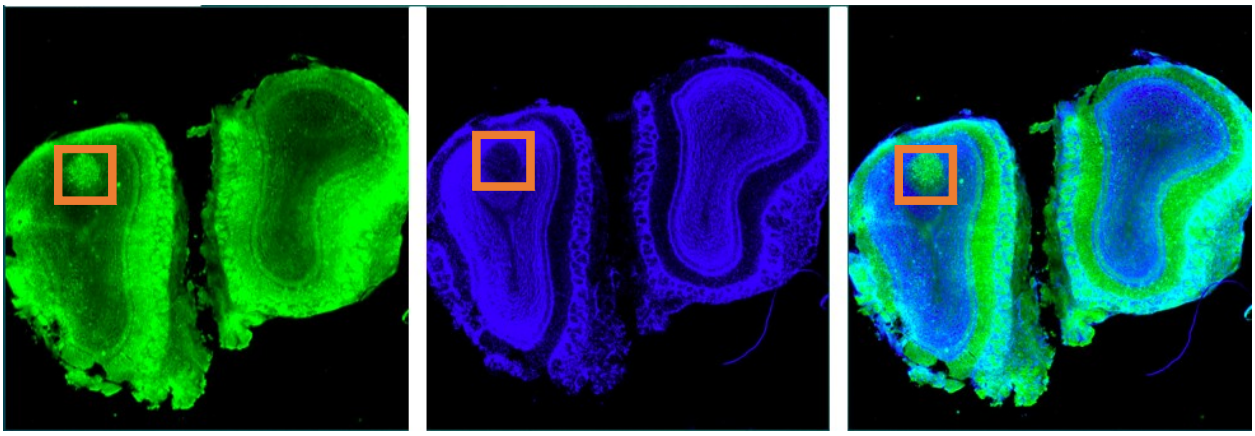

Figure 8: Representative histology sections from Tbet-cre mice injected with the GCaMP7F Cre-dependent virus. Cell nuclei were stained with a DAPI solution. Images were obtained with a fluorescence microscope using both GFP and DAPI channels. A. Image of the left olfactory bulb. The bottom panel represents a close up of the section in the top panel. The black line outlines the mitral cell layer, which expresses the Cre-recombinase protein. Fluorescence was expected to be confined to that region. Instead, it is concentrated towards the edge, which led us to conclude that we are observing background fluorescence. B. Image of the left and right olfactory bulb for comparison. There is no significant difference in GCaMP expression between both side even though the virus was injected in the left olfactory bulb. The orange box highlights an area that could be the injection site or where the bulb may have been fried.

Verification of GCaMP6f expression in Tbet-cre-Ai148D mice

We did not inject any virus in our third strain of mice because, as previously mentioned, they encode the *GCaMP6f* gene in their genome. Similar to Tbet-cre mice, Tbet-Cre-Ai148D mice only exhibited background fluorescence (figure 9). We did not see expression of GCaMP in the mitral layer as expected, but rather towards the edges of the olfactory bulb sections, which is not the region expressing the Cre recombinase protein. These mice never received doxycycline and thus expressed GCaMP all their lives. It is possible that the continuous fluorescence may have fried the bulb, which explains why we do not see GCaMP expression. Overall, expression of GCaMP in the mouse examined was not successful.

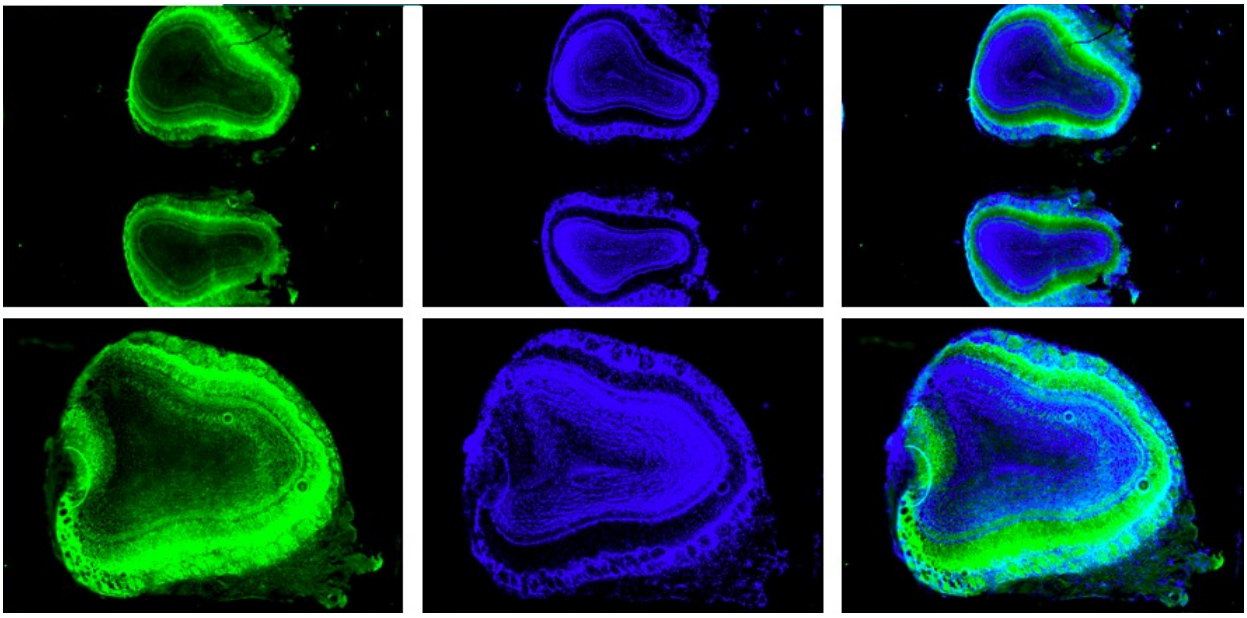

Figure 9: Representative histology sections from Tbet-Cre-Ai148D mice expressing GCaMP6F in their genome. Cell nuclei were stained with a DAPI solution. Images were obtained with a fluorescence microscope using both GFP and DAPI channels. Fluorescence is not confined to the mitral cell layer but is concentrated towards the edge of the section. Once again, we are observing background fluorescence and not real GCaMP expression.

Visualization of GCaMP expression via 2-photon microscopy

While we did histology on some mice to confirm expression of our fluorescence protein, we performed cranial window surgeries on others to directly observe activity using our imaging set-up. We ran across multiple issues with the imaging set-up. Sometimes, it did not work and we had to spend days or weeks recalibrating it or fixing whatever issues it had. Sometimes, the surgery was done poorly and the window was not clear. Other times, we did not place the head bar correctly and thus struggled to head fix the animal to image properly. When the set-up was working and the cranial window surgery seemed successful, we could not see any expression with the two-photon microscope, possibly because the virus injection surgery was not successful. There were days, however, when everything worked well, and we could visualize activity in the glomeruli. Figure 10 is a representative image from a mouse in which the surgeries

were successful, and the imaging set-up functioned properly. The 2-photon microscope has high resolution and allows some details of the cells. In the image, we can see cell bodies 9 (blue arrows) and axons or dendrites (orange arrows). This image was taken while the mouse was allowed to breathe normally. It was not exposed to any odorants. We also took videos where we could observe modulation of specific cells. This mouse represents one of the few successful results we had. We are continuing to adjust our surgical and imaging techniques in order to improve our success rate.

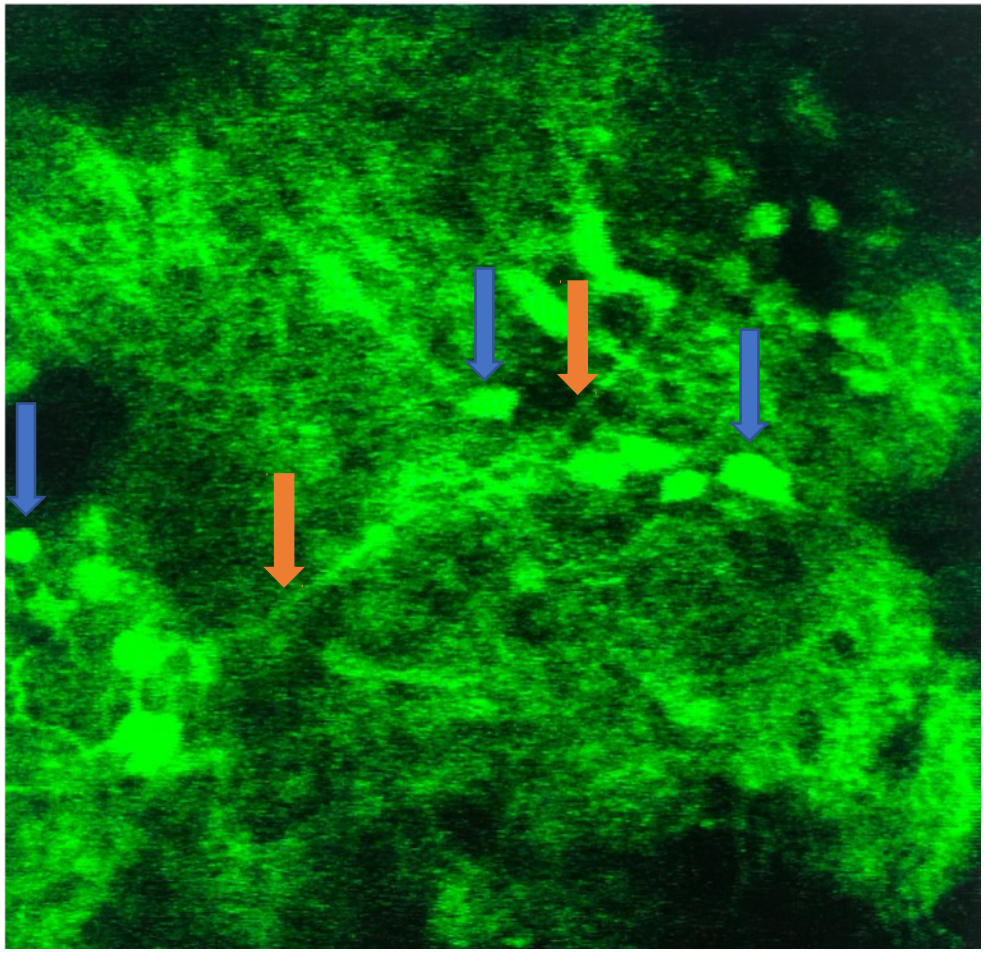

Figure 10: Representative image from a mice in which the surgeries were successful. The image was taken with a 2-photon microscope, which has high resolution. The orange arrows points to dendrites or axons while the blue arrows point to cell bodies.

Discussion:

The goal of our project was to establish a 2-photon imaging technique by addressing all the issues that arose with our imaging set-up and the multiple surgeries. Using the fluorescent dye DIO, we identified issues with our virus injection set-up and decided to switch to a different type of injection syringe. Histology from representative Tbet-cre and Tbet-Cre-Ai148D mice did not show any significant fluorescence, and we suspected it might have resulted from a frying of the olfactory bulb, or the degradation of the virus, in the case of Tbet-cre mice. We plan to do more histology shortly after injections (for Tbet-cre mice) or right after we stop feeding them doxycycline (for the Tbet-Cre-Ai148D). Sections from B6 mice did show some fluorescence, although not as much as expected. Despite the difficulty of cranial window surgeries, we were able to observe brain activity with the two-photon microscope in a live mouse. Nevertheless, the success rate remains low.

Although we have made significant progress since we started, we still have a long way to go. One of the things we decided to try was doing the cranial window surgeries more slowly and performing one or two surgeries at a time because we found out that being rushed or doing too many at a time reduced our success rate. We have also switched to larger windows because they were easier to place on the skull. Last year we tried injecting the virus at different locations and depths in the olfactory bulb to determine what was optimal, but we never looked at those mice because the cranial window surgeries were unsuccessful. Thus, our ability to make this technique work significantly depends on our perfecting of that surgical procedure. Future experiments will also involve exposing the mouse to different odorants and visualizing glomerular responses. Most of the data gathered during the project were from mice exposed to air.

Upon successful development and enhancement of the technique, the lab will move on to study how incoming signals shape the structure of navigational behavior. We will use this technique to test the hypothesis that olfactory navigation is driven by comparison of glomerular signals across multiple sniffs. Our first aim is to determine how navigating an odor gradient drives glomerular activity. We will monitor olfactory input to the brain by combining our behavioral assay with imaging. Genetically-encoded indicators will be expressed in the olfactory bulb, and a wireless-capable, lightweight, head-mounted microscope will capture glomerular signals. We hypothesize that the structure of navigation behavior depends on sniff-to-sniff comparison of sensory input. This hypothesis predicts that the movement structure will depend on both the recent sniffs and changes between successive sniffs.

Our second aim is to determine how glomerular activity drives navigation in a fictive odor plume. For this purpose, we will optically activate opsin-expressing glomeruli to create fictive odor plume. This will enable us to map a causal link between glomerular activity and navigation behavior. We hypothesize that the mouse's next movement will be influenced by stimulation history and not just the most recent sniff. These experiments will enable us to study both how behavior impacts neural activity but also how neural activity drives subsequent behavior.

Mouse olfactory navigation behavior provides an excellent opportunity to study active sensing because olfaction is inherently active, as odor access to the nose is gated by respiration. Additionally, navigating to an odor source requires active nose movement to collect odor samples across space and time. Our lab will use these strategies to study how olfactory sampling, and active sensing in general, drives natural behavior such as foraging, courtship, and predator

avoidance. In doing so, we will develop a better understanding of active sensory sampling behavior, which is disrupted in disorders such as autism and schizophrenia.

Bibliography:

Bhattacharyya, U., Singh Bhalla, U., 2015. Robust and rapid air borne odor tracking without casting. eNeuro 1–67. doi:10.1523/ENEURO.0102-15.2015

Catania, Kenneth C. "Stereo and Serial Sniffing Guide Navigation to an Odour Source in a Mammal." *Nature Communications*, vol. 4, no. 1, 2013, doi:10.1038/ncomms2444.

Croy et al. Olfaction as a Marker for Depression in Humans. *Journal of Affective Disorders*, Elsevier, 4 Jan. 2014, www.sciencedirect.com/science/article/pii/S0165032713008665

Dana, H., Sun, Y., Mohar, B., Hulse, B., Hasseman, J. P., Tsegaye, G., … Kim, D. S. (2018). High-performance GFP-based calcium indicators for imaging activity in neuronal populations and microcompartments. *Nature Methods*. doi: 10.1101/434589

Daigle, T. L., Madisen, L., Hage, T. A., Valley, M. T., Knoblich, U., Larsen, R. S., … Zeng, H. (2018). A Suite of Transgenic Driver and Reporter Mouse Lines with Enhanced Brain-Cell-Type Targeting and Functionality. *Cell*, *174*(2). doi: 10.1016/j.cell.2018.06.035

DiO perchlorate [3,3-Dioctadecyloxacarbocyanine perchlorate]: AAT Bioquest. (n.d.). Retrieved from https://www.aatbio.com/products/dio-perchlorate-3-3-dioctadecyloxacarbocyanine-perchlorate

Doty, R. L., Brugger, W. E., Jurs, P. C., & Orndorff, M. A. (1978). Intranasal trigeminal stimulation from odorous volatiles: psychometric responses from anosmic and normal humans. *Physiology & Behavior*, *20*(2), 175–185. http://doi.org/10.1016/0031-9384(78)90070-7

Hurst, J.L., Beynon, R.J., 2004. Scent wars: the chemobiology of competitive signalling in mice. Bioessays 26, 1288–1298. doi:10.1002/bies.20147

Irit Gazit, and Joseph Terkel. Domination of Olfaction over Vision in Explosives Detection by Dogs. *Applied Animal Behaviour Science*, Elsevier, 28 Mar. 2003, www.sciencedirect.com/science/article/pii/S0168159103000510

Johnson, B.A., Leon, M., 2007. Chemotopic odorant coding in a mammalian olfactory system. J. Comp. Neurol. 503, 1–34. doi:10.1002/cne.21396

Jones, Peter W, and Nathan N Urban. "Mice Follow Odor Trails Using Stereo Olfactory Cues and Rapid Sniff to Sniff Comparisons." 2018, doi:10.1101/293746

Kass, M.D., Rosenthal, M.C., Pottackal, J., McGann, J.P., 2013. Fear learning enhances neural responses to threat-predictive sensory stimuli. Science 342, 1389–1392. doi:10.1126/science.1244916

Kato, H.K., Chu, M.W., Isaacson, J.S., Komiyama, T., 2012. Dynamic Sensory Representations in the Olfactory Bulb: Modulation by Wakefulness and Experience. Neuron 76, 962–975. doi:10.1016/j.neuron.2012.09.037

Khan, A.G., Sarangi, M., Bhalla, U.S., 2012. Rats track odour trails accurately using a multi-layered strategy with near-optimal sampling. Nature Communications 3, 703–703. doi:10.1038/ncomms1712

Lerman, Gilad M, et al. "Precise Optical Probing of Perceptual Detection." 2018, doi:10.1101/456764.

Luo, Fang, et al. "Genetically Encoded Neural Activity Indicators." *Brain Science Advances*, vol. 4, no. 1, Nov. 2018, pp. 1–15., doi:10.26599/bsa.2018.9050007.

Meister, M., Bonhoeffer, T., 2001. Tuning and topography in an odor map on the rat olfactory bulb. Journal of Neuroscience 21, 1351–1360.

Mori, K. The Olfactory Bulb: Coding and Processing of Odor Molecule Information. *Science*, vol. 286, no. 5440, 1999, pp. 711–715., doi:10.1126/science.286.5440.711.

Neunuebel, J.P., Taylor, A.L., Arthur, B.J., Egnor, S.E.R., 2015. Female mice ultrasonically interact with males during courtship displays. eLife 4, 752. doi:10.7554/eLife.06203

O'Connor, D.H., Clack, N.G., Huber, D., Komiyama, T., Myers, E.W., Svoboda, K., 2010. Vibrissa-Based Object Localization in Head-Fixed Mice. Journal of Neuroscience 30, 1947–1967. doi:10.1523/JNEUROSCI.3762-09.2010

Overview. (n.d.). Retrieved from https://www.jax.org/strain/030328

Parabucki, A., Bizer, A., Morris, G., Smear, M. C., & Shusterman, R. (2017). Odor concentration change detectors in the Olfactory Bulb. *bioRxiv*, 114520.

Shusterman, R., Smear, M. C., Koulakov, A. A., & Rinberg, D. (2011). Precise olfactory responses tile the sniff cycle. *Nature Neuroscience*, *14*(8), 1039–1044. http://doi.org/10.1038/nn.2877

Smear, Matthew, et al. "Multiple Perceptible Signals from a Single Olfactory Glomerulus." *Flavour*, vol. 3, no. S1, Sept. 2013, doi:10.1186/2044-7248-3-s1-o11.

Soucy, E.R., Albeanu, D.F., Fantana, A.L., Murthy, V.N., Meister, M., 2009. Precision and diversity in an odor map on the olfactory bulb. Nat Neurosci 12, 210–220. doi:10.1038/nn.2262

Spors, H., Grinvald, A., 2002. Spatio-temporal dynamics of odor representations in the mammalian olfactory bulb. Neuron 34, 301–315.

Stewart, W.B., Kauer, J.S., Shepherd, G.M., 1979. Functional organization of rat olfactory bulb analyzed by the 2-deoxyglucose method. J. Comp. Neurol. 185, 715–734. doi:10.1002/cne.901850407

Wallace, D.J., Greenberg, D.S., Sawinski, J., Rulla, S., Notaro, G., Kerr, J.N.D., 2013. Rats maintain an overhead binocular field at the expense of constant fusion. Nature 1–6. doi:10.1038/nature12153

Wesson, D.W., Verhagen, J.V., Wachowiak, M., 2009. Why sniff fast? The relationship between sniff frequency, odor discrimination, and receptor neuron activation in the rat. J Neurophysiol 101, 1089–1102. doi:10.1152/jn.90981.2008

Wilson, R. I., & Mainen, Z. F. (2006). Early Events In Olfactory Processing. *Annual Review of Neuroscience*, *29*(1), 163–201. doi: 10.1146/annurev.neuro.29.051605.112950

Zepper, M. (2008, January 30). Floxing. Retrieved from https://en.wikipedia.org/wiki/Floxing